R.J. Marks II, "Two-dimensional coherent space-variant processing using temporal holography", Applied Optics, vol. 18, pp.3670-3674 (1979).

Two-dimensional coherent space-variant processing using temporal holography: processor theory

Robert J. Marks II

Using the temporal integration and summation properties of the conventional transmission hologram in conjunction with some recently developed linear operator characterizations, a number of coherent processors are developed which are capable of performing generalized 2-D linear space-variant operations.

I. Introduction

There have been many recent attempts to perform generalized linear space-variant operations with coherent processors. Deen *et al.*[1] have suggested angle multiplexing a number of responses within the emulsion of a volume hologram. This method has been shown to be ineffective due to undesirable Bragg diffraction geometry.[2] A second multiplexing method, suggested by Krile *et al.*,[3] makes use of phase-coded reference beams. In this scheme, a degree of diffuse background noise due to crosstalk terms is always present in the processor output.

Francois and Carlson[4] have investigated the class of space-variant operations achievable by N arbitrarily spaced planar amplitude transmittances. They have recently shown that all such processor operations can be expressed in terms of a number of cascaded multiplication-Fourier transform stages.[5] These are operations which can be achieved by conventional coherent processors.

Many space-variant operations can be decomposed into a coordinate distortion followed by space-invariant or Fourier transform operations.[6–8] Bryngdahl[9] has presented a scheme for performing a large class of such distortions. The method, however, imposes a rather severe space–bandwidth product on the input.[7]

If one is willing to sacrifice a dimension, the 1-D processors of Rhodes and Florence,[10,11] Goodman *et al.*,[12] and Marks *et al.*[13,14] are recommended.

This paper presents a number of generalized 2-D space-variant coherent processors. Each makes use of the temporal field amplitude summation/integration capabilities of the conventional transmission hologram,[15–18] which, for purposes of completeness and continuity, are briefly reviewed in Appendix A. The use of photosensitive media for performing summation of *incident light intensities* has been utilized previously in incoherent processing. The interested reader is referred to the excellent review paper by Monahan *et al.*[19]

The author is with University of Washington, Department of Electrical Engineering, Seattle, Washington 98195.

Received 6 April 1979.
0003-6935/79/213670-05$00.50/0.

II. Two-Dimensional Space-Variant Processors using Temporal Holography

The output, $g(x,y)$, of a 2-D linear space-variant system corresponding to an input, $u(\xi,\eta)$, can be written as

$$g(x,y) = \iint_{-\infty}^{\infty} u(\xi,\eta)h(x-\xi,y-\eta;\xi,\eta)d\xi d\eta, \quad (1)$$

where the linear operation's point-spread function (impulse response) h is given by the system response to an input Dirac delta point source. We here are using the Lohmann-Paris point-spread function notation.[20,21] Three methods of characterization of the superposition integral in Eq. (1) are discussed in detail in Ref. 22. A brief review of these characterizations in two dimensions is offered in Appendix B.

We now present a number of coherent processors that are capable of performing Eq. (1). Each processor requires a mask with real time transmittance changing capability (either mechanically or electrically) as well as a means of sequential data input. These processors are not meant to be representative of all possible cases, but rather are illustrative of a basic methodology.

A. Type 1 Processors

The recording and playback geometries for the processor we shall refer to as type 1 are pictured in Fig. 1. Both recording and playback geometries consist of the conventional two-lens convolution (space-invariant

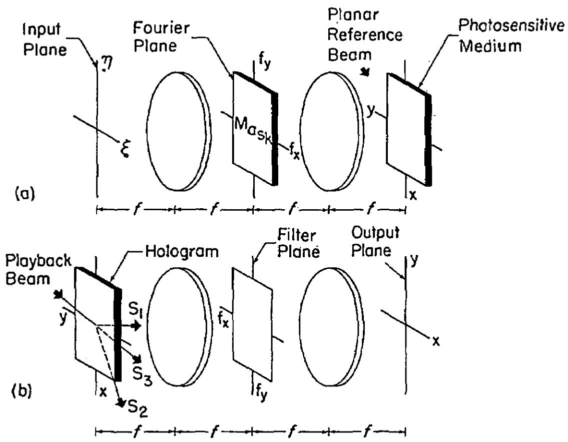

Fig. 1. The (a) recording and (b) playback geometries of the type 1 processor.

operation) processor. The addition of the dimension of time allows for performance of space-variant operations.

In the Fourier and filter planes of Fig. 1, the spatial frequency variables, f_x and f_y, are determined by dividing the corresponding spatial displacement by λf, where λ is the wavelength of the coherent illumination and f refers to the lens focal length.[15]

Implementation of some specific space-variant operation characterizations follows.

1. *Sampling Theorem Approach: Sequential Exposure*

To implement the sampling theorem for space-variant systems, sample input values, $u(\xi_n,\eta_m)\delta(\xi - \xi_n,\eta - \eta_m)$, are sequentially input into the system. [$\delta(\xi - \xi_n,\eta - \eta_m)$ refers to a unit Dirac delta or point source located at coordinates (ξ_n,η_m) on the input plane.] Using a scanner, this can be achieved by either placing the transmittance $u(\xi,\eta)$ on the input plane or by amplitude modulation of the scanner beam.

In either case, the input is Fourier transformed, and the field amplitude incident on the Fourier plane is

$$u(\xi_n,\eta_m)\exp[-j2\pi(f_x\xi_n + f_y\eta_m)]. \quad (2)$$

For the nmth exposure, we place a mask with the amplitude transmittance $H(f_x,f_y;\xi_n,\eta_m)$ in the Fourier plane, where

$$H(f_x,f_y;\xi_n,\eta_m) = \iint_{-\infty}^{\infty} h(x,y;\xi_n,\eta_m)\exp[-j2\pi(f_x x + f_y y)]dxdy. \quad (3)$$

The mask is recognized as a sample transfer function of the desired space-variant operation.

The field amplitude immediately to the right of the Fourier plane is given by the product of $H(f_x,f_y;\xi_n,\eta_m)$ and Eq. (2). This product is again Fourier transformed to give incident on the photosensitive medium the sum of the planar reference beam field amplitude and

$$u(\xi_n,\eta_m)h(x - \xi_n,y - \eta_m;\xi_n,\eta_m). \quad (4)$$

After making a number of such exposures, the resulting hologram is placed in the playback geometry of Fig. 1(b). Upon illumination with the playback beam, the diffracted term of interest (denoted by s_1) is

$$\sum_n \sum_m u(\xi_n,\eta_m)h(x - \xi_n,y - \eta_m;\xi_n,\eta_m). \quad (5)$$

(We here and henceforth will assume that the unwanted diffracted terms, s_2 and s_3 in Fig. 1, are propagating at sufficiently steep angles to miss the transforming lens. If such is not the case, they can be removed in many cases by placing an appropriate aperture in the filter plane.[13] This assumption is made so as not to confuse the filtering of s_1 from s_2 and s_3 with the low pass filtering required in the sampling theorem.)

If low pass filtering is required [see Eq. (B2)], an appropriate rectangular aperture is placed in the filter plane. Otherwise [Eq. (B3)], no filtering is required. In either case, the desired output appears on the processor's output plane.

2. *Second Sampling Theorem Approach: Raster Input Scanning*

In this scheme, $u(\xi,\eta)$ is input into the system via a raster scan. We denote the mth line scan by

$$u(vt;\eta_m)\delta(\xi - vt;\eta - \eta_m), \quad (6)$$

where v is the scanning speed. At time t, the field amplitude incident on the Fourier plane is

$$u(vt;\eta_m)\exp[-j2\pi(f_x vt + f_y\eta_m)]. \quad (7)$$

We assume that the mask has real-time amplitude transmittance changing capability, which, at time t, is $H(f_x,f_y;vt,\eta_m)$. The field amplitude to the right of the Fourier plane is the product of this transmittance and (7). This product is again Fourier transformed to give incident on the photosensitive medium the sum of the reference beam, and

$$u(vt;\eta_m)h(x - vt,y - \eta_m;vt,\eta_m). \quad (8)$$

If the exposure time for a single scan is T, the corresponding term in the resulting hologram is

$$\int_0^T |u(vt;\eta_m)h(x - vt,y - \eta_m;vt,\eta_m) + \exp(jk\alpha y)|^2 dt. \quad (9)$$

A number of such scans are made corresponding to various values of m. Upon illumination with the playback beam, the resulting hologram will yield a diffracted term (corresponding to s_1) of the form

$$\sum_m \int_0^T u(vt;\eta_m)h(x - vt,y - \eta_m;vt,\eta_m)dt$$
$$= \frac{1}{v}\sum_m \int_{-\infty}^{\infty} u(\xi,\eta_m)h(x - \xi,y - \eta_m;\xi,\eta_m)d\xi, \quad (10)$$

where we have made the variable substitution $\xi = vt$.

The desired aperture in the filter plane of Fig. 1(b) again depends on the form of the sampling theorem being implemented. If low pass filtering is required [Eq. (B2)], an appropriately dimensioned vertical slit is required. Otherwise [Eq. (B3)], no aperture is

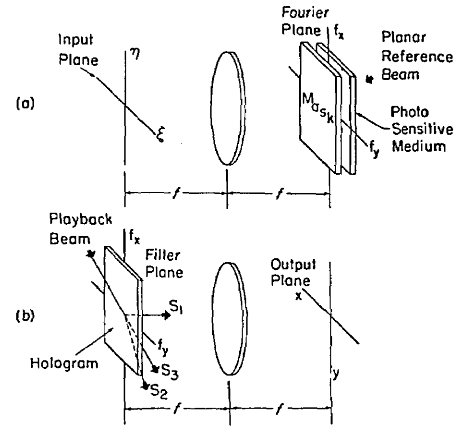

Fig. 2. The (a) recording and (b) playback geometries of the type 2 processor.

needed. In either case, the desired operation output, $g(x,y)$, appears on the processor's output plane.

3. Third Sampling Theorem Approach: Stationary Input Source

Here we consider the case where the input point source is always at the origin of the input plane. That is, the nmth input is of the form

$$u(\xi_n,\eta_m)\delta(\xi,\eta). \tag{11}$$

The corresponding field amplitude incident on the Fourier plane is simply $u(\xi_n,\eta_m)$. If we assume that the nmth mask transmittance is

$$H(f_x,f_y;\xi_n,\eta_m)\exp[-j2\pi(f_x\xi_n + f_y\eta_m)], \tag{12}$$

the field amplitude incident on the photosensitive medium is the sum of the planar reference beam and

$$u(\xi_n,\eta_m)h(x-\xi_n,y-\eta_m;\xi_n,\eta_m). \tag{13}$$

This is the same relation as (4). The procedure for playback is thus identical to that in Sec. II.A.1.

The stationary point source can also change continuously in time. In this case, the input is $u(vt,\eta_m)\delta(\xi,\eta)$, and the instantaneous mask transmittance for the mth scan is

$$H(f_x,f_y;vt,\eta_m)\exp[-j2\pi(vtf_x + \eta_m f_y)]. \tag{14}$$

The playback procedure is identical to that described in Sec. II.A.2.

4. PIA Implementation

The processor in Fig. 1 can also be used to implement the piecewise isoplanatic approximation (PIA) of Eq. (1). Here, an input transmittance, $u(\xi,\eta)$, is placed on the input plane. The nmth of the number of exposures made corresponds to unit coherent plane wave illumination of the nmth isoplanatically modeled input patch. The corresponding mask is $H(f_x,f_y;\xi_n,\eta_m)$, the same as was used in the sampling theorem implementation in Sec. II.A.1. The nmth field amplitude incident on the photosensitive medium is the sum of the planar reference beam and

$$\int_{k_n}^{k_{n+1}}\int_{l_n}^{l_{n+1}} u(\xi,\eta)h(x-\xi,y-\eta;\xi_n,\eta_m)d\xi d\eta. \tag{15}$$

By making a number of such exposures corresponding to all desired nm values, the resulting hologram, when placed in the playback geometry of Fig. 1(b), will generate the PIA of the linear operation (B1).

5. Sinc Response Implementation

The sinc response characterization in Eq. (B8) can also be implemented by the processor of Fig. 1. The scheme is identical to the sampling theorem implementation in Sec. II.A.1. except that (1) a Fourier mask transmittance of

$$\int^{\infty}\int_{-\infty} S[\mathrm{sinc}2W_x(\xi-\xi_n)\,\mathrm{sinc}2W_y(\eta-\eta_m)] \times \exp[-j2\pi(f_x x + f_y y)]dxdy \tag{16}$$

is used, and (2) no filtering is required in playback. The nmth Fourier mask corresponds to an input of $u(\xi_n,\eta_m)\delta(\xi-\xi_n,\eta-\eta_m)$.

One can also use a stationary input, $u(\xi_n,\eta_m)\delta(\xi,\eta)$ (as in the sampling theorem characterization in Sec. II.A.2), if the corresponding mask transmittance in Eq. (16) is multiplied by the phase term $\exp[-j2\pi(f_x\xi_n + f_y\eta_m)]$.

B. Type 2 Processors

The type 2 processor, pictured in Fig. 2, is similar in personality to the type 1 processor. The only difference is that recording and playback are performed on the frequency (f_x,f_y)-plane rather than the spatial (x,y)-plane.

C. Type 3 Processors

The type 3 processor, pictured in Fig. 3, can be utilized to implement either the sampling theorem or sinc response linear system characterization.

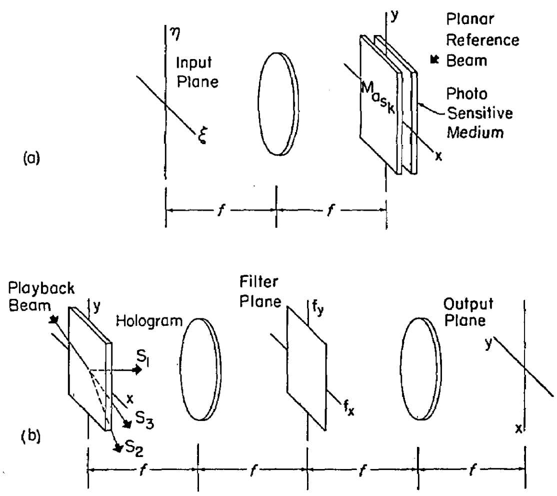

Fig. 3. The (a) recording and (b) playback geometries of the type 3 processor.

1. Sampling Theorem Approach

For sequential recording, our nmth input is $u(\xi_n,\eta_m)\delta(\xi,\eta)$. This yields a plane wave with field amplitude $u(\xi_n,\eta_m)$ incident on the mask. The nmth mask has a transmittance of $h(x-\xi_n,y-\eta_m;\xi_n,\eta_m)$. After a number of exposures, the diffraction term of interest from the resulting hologram is thus

$$\sum_n \sum_m u(\xi_n,\eta_m)h(x-\xi_n,y-\eta_m;\xi_n,\eta_m). \tag{17}$$

Filtering may or may not be required, depending on which sampling theorem [(B2) or (B3)] is applicable.

If the mask has continuous real-time amplitude changing capabilities, we could scan the input as was done in Sec. II.A.3.

2. Sinc Response Approach

The sinc response is implemented in the same fashion as the sequential sampling in the previous section, except that the nmth mask transmittance is the sinc response:

$$S[\mathrm{sinc}2W_x(\xi-\xi_n)\,\mathrm{sinc}2W_y(\eta-\eta_m)]. \tag{18}$$

No filtering is required.

III. Conclusions

A methodology has been presented whereby 2-D linear space-variant operations can be performed. A temporal integrating/summing hologram and a specific operation characterization are common to all.

There are three basic disadvantages to these processors: (1) sequential data input; (2) the requirement of changing masks; and (3) the decrease in SNR resulting when a number of exposures are stacked on a single hologram.

The processors do, however, demonstrate a feasible combination of temporal and spatially parallel processing which is capable of performing generalized 2-D linear space-variant operations.

This work was supported in part by the University of Washington Graduate Research Fund (project PSE-517).

Appendix A: Temporal Holography

The foundation of the processors in this paper rests on temporal holographic integration and summation operations. If a time-varying field amplitude, $a(x,y;t)$, is incident on a photosensitive medium paced on the (x,y) plane and $\exp(j\alpha ky)$ denotes a planar reference beam, the resulting intensity at time t is

$$I(x,y;t) = |a(x,y;t) + \exp(j\alpha ky)|^2. \tag{A1}$$

After processing, we make the conventional assumption that the corresponding hologram will have a field amplitude transmittance proportional to[15–17]

$$b(x,y) = \int_0^T I(x,y;t)dt = b_1 + b_2 + b_3, \tag{A2}$$

where T is the exposure time, and

$$\left.\begin{aligned} b_1(x,y) &= \int_0^T a(x,y;t)dt\,\exp(-j\alpha ky) \\ b_2(x,y) &= \bar{b}_1(x,y) \\ b_3(x,y) &= T + \int_0^T |a(x,y;t)|^2 dt \end{aligned}\right\}. \tag{A3}$$

The overbar denotes complex conjugation. Upon playback with the reference beam, three diffracted terms will emerge:

$$s_i(x,y) = b_i(x,y)\exp(j\alpha ky);\quad i = 1, 2, 3. \tag{A4}$$

The term corresponding to b_1 is the temporal integral of the original time-varying incident field amplitude:

$$s_1(x,y) = \int_0^T a(x,y;t)dt. \tag{A5}$$

Alternately, we could have exposed the photosensitive medium to N time-varying field amplitudes, $a_n(x,y;t)$, $n = 1, 2, \ldots, N$. In this case the corresponding diffracted term is of the form

$$s_1(x,y) = \sum_{n=1} \int_0^T a_n(x,y;t)dt. \quad \text{(A6)}$$

Thus, the hologram can act as an integrator and/or summer of incident time-varying field amplitudes.

Appendix B: Linear Space-Variant System Characterizations

A. Piecewise Isoplanatic Approximation

In the piecewise isoplanatic approximation (PIA), the input plane is divided into isoplanatically modeled patches, the nmth of which is described by $k_n \leq \xi < k_{n+1}$ and $l_m \leq \eta < l_{m+1}$. Then

$$g(x,y) \approx \sum_n \sum_m \int_{k_n}^{k_{n+1}} \int_{l_n}^{l_{m+1}} u(\xi,\eta)h(x-\xi,y-\eta;\xi_n,\eta_m)d\xi d\eta, \quad \text{(B1)}$$

where we choose the coordinate (ξ_n,η_n) such that $k_n \leq \xi_n \leq k_{n+1}$ and $l_m \leq \xi_m \leq l_{m+1}$. Here, the superposition integral is reduced to a sum of convolutions. The calibration of the input plane is independent of the input.

B. Space-Variant System Sampling Theory

Classical Shannon sampling theory is applicable to linear system characterization. If certain bandlimited constraints are placed on the input and impulse response,

$$g(x,y) = \sum_n \sum_m u(\xi_n,\eta_m)h(x-\xi_n,y-\eta_m;\xi_n,\eta_m) * \text{sinc}2B_x x \,\text{sinc}2B_y y, \quad \text{(B2)}$$

where $\xi_n = \eta/2B_x$, $\eta_m = m/2B_y$, $\text{sinc}x = \sin\pi x/\pi x$, and "$*$" denotes convolution. The sampling rates, $2B_x$ and $2B_y$, are determined by both the input's and the impulse response's bandwidths.

Under alternate bandlimiting constraints, the convolving sincs in (9) are unnecessary. That is,

$$g(x,y) = \frac{1}{4\hat{B}_x\hat{B}_y} \sum_n \sum_m u(\xi_n,\eta_m)h(x-\xi_n,y-\eta_m;\xi_n,\eta_m), \quad \text{(B3)}$$

where, now, $\xi_n = n/2\hat{B}_x$ and $\eta_m = m/2\hat{B}_y$. The sampling rates here, $2\hat{B}_x$ and $2\hat{B}_y$, are also dependent on the input and impulse response.

C. Orthonormal Basis Set Response Characterization

Limiting our input to that class of signals spanned by a 2-D orthonormal basis set $[\phi_{nm}(\xi,\eta)]$, we can write

$$u(\xi,\eta) = \sum_n \sum_m \alpha_{nm}\phi_{nm}(\xi,\eta), \quad \text{(B4)}$$

where

$$\alpha_{nm} = \int_{-\infty}^{\infty} u(\xi,\eta)\overline{\phi}_{nm}(\xi,\eta)d\xi d\eta. \quad \text{(B5)}$$

In this case, the system output is given by

$$g(x,y) = \sum_n \sum_m \alpha_{nm} S[\phi_{nm}(\xi,\eta)], \quad \text{(B6)}$$

where $S[\phi_{nm}(\xi,\eta)]$ denotes the linear system's response to an input $\phi_{nm}(\xi,\eta)$:

$$S[\phi_{nm}(\xi,\eta)] = \int^{\infty} \int_{-\infty} \phi_{nm}(\xi,\eta)h(x-\xi,y-\eta;\xi,\eta)d\xi d\eta. \quad \text{(B7)}$$

Note that this method of system characterization depends only on the input class.

As an example, consider the case where the input class consists of all finite energy signals with xy-bandwidths less than $2W_x$ and $2W_y$, respectively. We can apply the conventional Whittaker-Shannon sampling theorem[15] and write

$$g(x,y) = \sum_n \sum_m u(\xi_n,\eta_m)S[\text{sinc}2W_x(\xi-\xi_n)\,\text{sinc}2W_y(\eta-\eta_m)], \quad \text{(B8)}$$

where $\xi_n = n/2W_x$ and $n_m = m/2W_y$. Thus the system is characterized by its sinc response set and the sample values of the input.

References

1. L. M. Deen, J. F. Walkup, and M. O. Hagler, Appl. Opt. **14**, 2438 (1975).
2. R. J. Marks II, "Space-Variant Coherent Optical Processing," Scientific Report 1 on ASOFR grant 75-2855 (Texas Tech. University), Department of Electrical Engineering, Lubbock (December 1977).
3. T. F. Krile, R. J. Marks II, J. F. Walkup, and M. O. Hagler, Appl. Opt **16**, 3131 (1977).
4. F. P. Carlson and R. E. Francois, Jr., Proc. IEEE **65**, 10 (1977).
5. R. E. Francois, Jr. and F. P. Carlson, Appl. Opt. **18**, 2775 (1979).
6. A. A. Sawchuk, J. Opt. Soc. Am. **64**, 138 (1974).
7. J. W. Goodman, Proc. IEEE **65**, 29 (1977).
8. D. Casasent and D. Psaltis, Proc. IEEE **65**, 77 (1977).
9. O. Bryngdahl, J. Opt. Soc. Am. **64**, 1092 (1974).
10. W. T. Rhodes and J. Florence, Appl. Opt. **15**, 3073 (1976).
11. J. M. Florence, "Frequency-Variant Optical Signal Processing," Ph.D. Thesis, Georgia Institute of Technology, Atlanta (January 1979).
12. J. W. Goodman, P. Kellman, and E. W. Hansen, Appl. Opt. **16**, 733 (1977).
13. R. J. Marks II, J. F. Walkup, M. O. Hagler, and T. F. Krile, Appl. Opt. **16**, 739 (1977).
14. R. J. Marks II, M. I. Jones, E. L. Kral, and J. F. Walkup, Appl. Opt. **18**, 2783 (1979).
15. J. W. Goodman, *Introduction to Fourier Optics* (McGraw-Hill, New York, 1968).
16. J. W. Goodman, Appl. Opt. **6**, 857 (1967).
17. R. J. Collier, C. B. Burckhardt, and L. H. Lin, *Optical Holography* Academic, New York, 1971).
18. M. O. Hagler, E. L. Kral, J. F. Walkup, and R. J. Marks II, "Linear Coherent Processing Using an Input Scanning Technique," in *Proceedings International Optical Computing Conference*, London, England (1978).
19. M. A. Monahan, K. Bromley, and R. P. Bocker, Proc. IEEE **65**, 121 (1977).
20. A. W. Lohmann and D. P. Paris, J. Opt. Soc. Am. **55**, 1007 (1965).
21. R. J. Marks II, J. F. Walkup, and M. O. Hagler, Appl. Opt. **15**, 2289 (1976).
22. R. J. Marks II, J. F. Walkup, and M. O. Hagler, Appl. Opt. **18**, 655 (1979).